Impaired lymphatic contraction associated with immunosuppression

Shan Liao[a], Gang Cheng[a], David A. Conner[b], Yuhui Huang[a], Raju S. Kucherlapati[b], Lance L. Munn[a], Nancy H. Ruddle[c], Rakesh K. Jain[a,1], Dai Fukumura[a,1], and Timothy P. Padera[a,1]

[a]E. L. Steele Laboratory, Department of Radiation Oncology, Harvard Medical School and Massachusetts General Hospital, Boston, MA 02114; [b]Department of Genetics, Brigham and Women's Hospital, Boston, MA 02115; and [c]Departments of Epidemiology and Public Health and Immunobiology, Yale University School of Medicine, New Haven, CT 06511

Contributed by Rakesh K. Jain, October 6, 2011 (sent for review September 10, 2011)

To trigger an effective immune response, antigen and antigen-presenting cells travel to the lymph nodes via collecting lymphatic vessels. However, our understanding of the regulation of collecting lymphatic vessel function and lymph transport is limited. To dissect the molecular control of lymphatic function, we developed a unique mouse model that allows intravital imaging of autonomous lymphatic vessel contraction. Using this method, we demonstrated that endothelial nitric oxide synthase (eNOS) in lymphatic endothelial cells is required for robust lymphatic contractions under physiological conditions. By contrast, under inflammatory conditions, inducible NOS (iNOS)-expressing CD11b$^+$Gr-1$^+$ cells attenuate lymphatic contraction. This inhibition of lymphatic contraction was associated with a reduction in the response to antigen in a model of immune-induced multiple sclerosis. These results suggest the suppression of lymphatic function by the CD11b$^+$Gr-1$^+$ cells as a potential mechanism of self-protection from autoreactive responses during on-going inflammation. The central role for nitric oxide also suggests that other diseases such as cancer and infection may also mediate lymphatic contraction and thus immune response. Our unique method allows the study of lymphatic function and its molecular regulation during inflammation, lymphedema, and lymphatic metastasis.

Inflammation and cancer dissemination share many features that result in alterations of both the structure and the function of lymphatic vessels, including lymphangiogenesis and vessel dilation (1–6). Although lymphangiogenesis and vessel dilation are thought to increase the delivery of lymph to the draining lymph node, a decrease in drainage has also been observed during inflammation and surrounding some cancers (1, 2, 7). Whether reductions in collecting lymphatic function can affect subsequent immune response by limiting entry of antigen/dendritic cells (DCs) into the draining lymph node (LN) is not known.

Lymph flow—a critical determinant of antigen and dendritic cell transport—is determined by a combination of lymph production and active and passive forces on collecting lymphatic vessels (8, 9). Collecting lymphatic vessels can produce flow autonomously using smooth muscle cell (SMC)-driven contractions, which drive flow through one-way intraluminal valves and lymph nodes before its return to the blood circulation (10). Although studies of lymphatic pumping in large animals have given insights into lymphatic contraction (11–15), molecular control of this process is not well understood. Given the ready availability of molecular reagents, genetic knockouts, and disease models in mice, an in vivo murine model of lymphatic contraction will advance the field by dissecting the underlying molecular mechanisms under normal and pathological conditions. Here, we demonstrate a unique murine model of autonomous collecting lymphatic contraction to study its regulation during inflammation and its impact on immune response.

Results

Real-Time Intravital Microscopy of Mouse Popliteal Lymphatic Vessel Contraction. To characterize the molecular regulation of lymphatic function, we developed a unique experimental mouse model that permits imaging of the afferent lymphatic vessel to the popliteal lymph node (PLV) (Fig. S1*A*). We observed axial propagation of lymphatic contraction and valve motion consistently for >1 h (*Materials and Methods* and Movies S1 and S2). Using mice that express *DsRed* in vascular SMCs under the control of the α-smooth muscle actin gene promoter (*αSMA^P-DsRed*), we verified that the observed PLV contractions are due to autonomous lymphatic contraction and are independent of blood vessel and skeletal muscle movements (Fig. 1*A* and Movies S3 and S4). Using quantitative image analysis to measure the vessel diameter as a function of time, we calculated the lymphatic ejection fraction (EF) and theoretical lymphatic output, which are analogous to parameters used to describe cardiac function. We used ejection fraction—the percentage of total volume ejected per contraction—to quantify the strength of lymphatic contraction.

We next tested the effects of nitric oxide (NO) on lymphatic contraction. NO is a known mediator of blood vessel tone and is produced by three isoforms of nitric oxide synthase (NOS): endothelial NOS (eNOS), inducible NOS (iNOS), and neuronal NOS (nNOS) (16). NO also mediates lymphatic function and lymphatic contraction (13, 17–23) and eNOS is expressed by collecting lymphatic vessels (Fig. S1*B*). We blocked NO production pharmacologically using the NOS inhibitor N^G-monomethyl-L-arginine monoacetate (L-NMMA) and genetically using *eNOS*$^{-/-}$ mice and found attenuated lymphatic contraction strength compared with that in wild-type (WT) control mice (Fig. 1 *B* and *C* and Movies S5, S6, S7, and S8). These data are consistent with reduced lymph flow shown previously in *eNOS*$^{-/-}$ mice (20) and in ex vivo preparations with pharmacological blockade (13, 17), although the latter findings are context dependent (16, 18, 22, 24). Furthermore, we saw an increase in contraction frequency in *eNOS*$^{-/-}$ mice (Fig. 1*C*), consistent with published work on the pacemaker activity of collecting lymphatic vessels (18, 25). Lymphatic contraction in *iNOS*$^{-/-}$ mice was no different from that in WT mice (Movie S9), also consistent with previous data (18). However, there was no significant difference in the overall lymphatic output among all these conditions (*Discussion* and *SI Materials and Methods*).

Attenuated Lymphatic Contraction During Inflammation. We next determined how lymphatic contraction is altered under inflammatory conditions. Skin contact sensitization using oxazolone

Author contributions: S.L., G.C., Y.H., L.L.M., N.H.R., R.K.J., D.F., and T.P.P. designed research; S.L., G.C., Y.H., N.H.R., and T.P.P. performed research; S.L., G.C., D.A.C., R.S.K., L.L.M., and T.P.P. contributed new reagents/analytic tools; S.L., G.C., Y.H., L.L.M., N.H.R., and T.P.P. analyzed data; and S.L., R.K.J., and T.P.P. wrote the paper.

Conflict of interest statement: R.K.J. received commercial research grants from Dyax, MedImmune, and Roche; consultant fees from Dyax, SynDevRx, Xtuit, and Noxxon Pharma; and a speaker honorarium from MPM Capital. R.K.J. owns stock in SynDevRx. No reagents or funding from these companies were used in these studies.

[1]To whom correspondence may be addressed. E-mail: jain@steele.mgh.harvard.edu, dai@steele.mgh.harvard.edu, or tpadera@steele.mgh.harvard.edu.

This article contains supporting information online at www.pnas.org/lookup/suppl/doi:10.1073/pnas.1116152108/-/DCSupplemental.

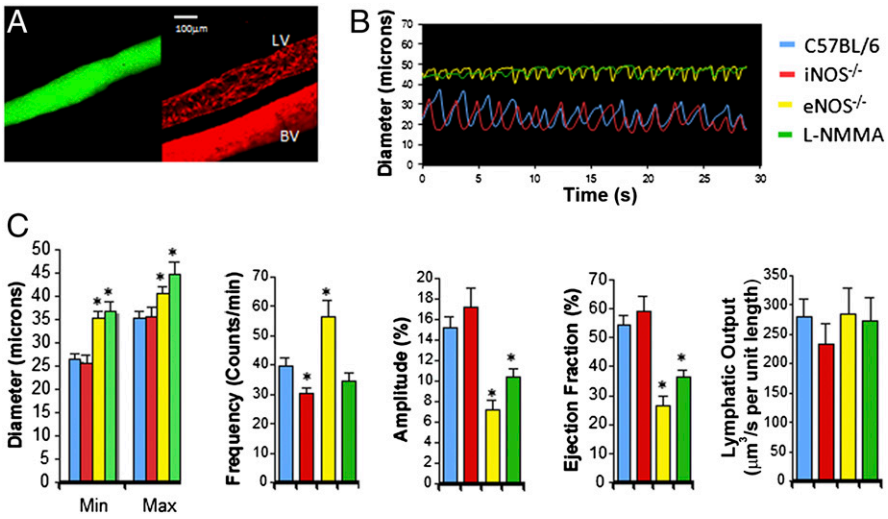

Fig. 1. Popliteal lymphatic vessels exhibit consistent pumping activity. (*A*) DsRed-labeled SMCs (*Right*) exhibit typical coverage of a lymphatic vessel (LV) identified by lymphangiography (*Left*, green). The adjacent blood vessel (BV) has greater smooth muscle cell coverage. (*B*) Representative lymphatic contraction curves show reduced contraction in $eNOS^{-/-}$ and L-NMMA–treated mice compared with WT and $iNOS^{-/-}$ mice. (*C*) Lymphatic contraction analyses of diameter, frequency, amplitude, ejection fraction, and lymphatic output. ■, C57BL/6, $n = 21$; ■, $iNOS^{-/-}$, $n = 14$; ■, $eNOS^{-/-}$, $n = 27$; ■, L-NMMA, $n = 11$. $^*P < 0.05$. *P* values are listed in Table S1. Error bars show SEM.

(OX) induces cutaneous inflammation with edema that begins 2 d after the induction, peaks on day 4 (OXd4), and resolves spontaneously by day 7 (2). On OXd4, we detected larger PLV diameters, abnormal SMC association, and reduced lymphatic ejection fraction (Fig. 2 *A* and *B*; Fig. S2*A*; and Movies S10, S11, and S12).

By immunofluorescence staining, we found that iNOS was expressed by the inflammatory cells, but not the collecting lymphatic vessel (Fig. S2*B*). As NO derived from *iNOS*-expressing lipopolysaccharide (LPS)-activated macrophages attenuates the contraction of myocytes and carotid arteries (26, 27), we hypothesized that lymphatic contraction is similarly attenuated by the overproduction of NO from *iNOS*-expressing inflammatory cells located in s.c. adipose tissue on OXd4 (Fig. 2*C*). On OXd4, both $eNOS^{-/-}$ and $iNOS^{-/-}$ mice had dilated lymphatic vessels compared with noninflammatory conditions (Fig. 2 *A* and *B* and Fig. S2*A*). However, we found that $iNOS^{-/-}$ mice maintained strong lymphatic contractions compared with WT (Fig. 2 *A* and *B*, Fig. S2*A*, and Movies S10 and S13). In contrast, the lymphatic contractions in $eNOS^{-/-}$ mice were weak at OXd4, similar to those in control mice (Fig. 2 *A* and *B*, Fig. S2*A*, and Movie S14).

To minimize the influence of the complex inflammatory microenvironment and to avoid complications of systemic NO blockade, we isolated macrophages from WT or $iNOS^{-/-}$ mice, activated them with LPS, and implanted them over the PLV in the absence of inflammation (Fig. S3*A*). Activated WT macrophages drastically increased iNOS expression (Fig. S3*B*) and after 2 h, significantly suppressed lymphatic contraction compared with those isolated from $iNOS^{-/-}$ mice (Fig. 2*D* and Fig. S3*C*). Macrophages isolated from both WT and $iNOS^{-/-}$ mice caused dilation of the lymphatic vessel, similar to the inflammatory condition. Interestingly, unlike in the inflammatory condition, we did not observe compensation for lymphatic output after the acute, local application of activated macrophages.

***iNOS*-Expressing Bone Marrow-Derived Cells Inhibit Lymphatic Contraction.** Using bone marrow transplants (BMTs) from $Actb^{P}$-*GFP* mice, we found that a large number of GFP^+ bone marrow-derived cells (BMDCs) infiltrate the tissue surrounding the PLV at OXd4 (Fig. 3*A*). Although $iNOS^{-/-}$ mice have dramatically reduced inflammation after OX sensitization (28), many inflammatory cells still accumulate in the inflamed leg at OXd4 (Fig. S2 *C* and *D*). To determine whether infiltrated cells directly suppress lymphatic contraction through iNOS, we performed BMT from WT to $iNOS^{-/-}$ mice and vice versa along with a transplantation control (WT to WT). As expected, there were no significant differences in lymphatic contraction between any of these chimera mice under physiological conditions, although all of them showed a reduced contraction strength compared with normal WT mice (Figs. 1*D* and 3*B* and *C* and Fig. S4*A*). This latter finding might be due to the irradiation or older age of the BMT mice (Fig. S5). After oxazolone skin painting, only WT mice with $iNOS^{-/-}$ bone marrow were able to continue robust contractions (Fig. 3 *B* and *D* and Fig. S4*B*). These results suggest that *iNOS*-expressing BMDCs inhibit lymphatic contraction during inflammatory conditions.

$CD11b^+Gr\text{-}1^+$ Cells Expressing *iNOS* Suppress Lymphatic Contraction. Sorting the cells into four populations ($CD45^+CD11b^+Gr\text{-}1^+$, $CD45^+$ $CD11b^+Gr\text{-}1^-F4/80^+$, $CD45^+Gr\text{-}1^-F4/80^-$, and $CD45^-$) and testing *iNOS* expression by quantitative RT-PCR, we found that the majority of *iNOS*-expressing cells were $CD45^+CD11b^+$ $Gr\text{-}1^+$ myeloid cells, which comprised 75 ± 3% of all infiltrated $CD45^+$ cells (Fig. S6*A*). By immunofluorescence staining, we confirmed that nearly all of the $Gr\text{-}1^+$ cells, along with some F4/80 macrophages, expressed iNOS (Fig. 4*A*). These iNOS-expressing cells were located close to the PLV (Fig. 4*A*). We next blocked the accumulation of $CD11b^+Gr\text{-}1^+$ myeloid cells using an anti-Gr-1 antibody. The anti-Gr-1 antibody treatment significantly restored lymphatic contraction compared with that in the IgG-treated control group at OXd4 (Fig. 4*B* and Fig. S6*B*). Thus, $CD11b^+$ $Gr\text{-}1^+$ cells expressing *iNOS* can inhibit autonomous lymphatic contraction during inflammation.

Reduced Antigen Accumulation in the Draining Lymph Node and Impaired T-Cell Response to Self-Antigen During Inflammation. Having identified the mechanism of attenuated lymphatic contraction during inflammation, we next investigated the immunological ramifications of our findings. To this end, we measured the kinetic response of lymphatic contraction, $Gr1^+$ cell accumulation, DC accumulation, and antigen-induced autoimmune disease after OX skin painting. The attenuation of lymphatic contraction over time is inversely related to $Gr1^+$ cell accumu-

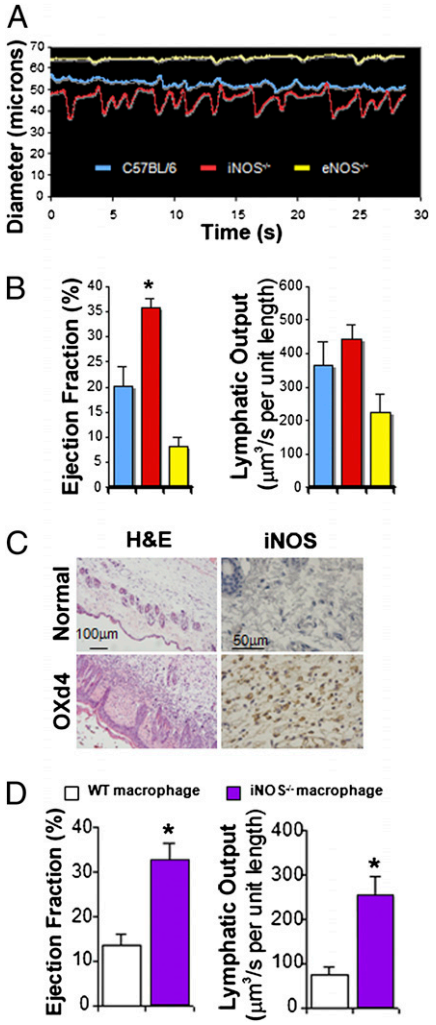

Fig. 2. Inflammation modulates lymphatic contraction through *iNOS*. (*A*) Representative lymphatic contraction curves for WT, $eNOS^{-/-}$, and $iNOS^{-/-}$ mice during inflammation. Only PLVs in $iNOS^{-/-}$ mice maintain strong contractions. (*B*) Lymphatic contraction analyses at day 4 after OX painting. ■, C57BL/6, $n = 14$; ■, $iNOS^{-/-}$, $n = 15$; ■, $eNOS^{-/-}$, $n = 9$. (*C*) Immunohistochemical staining shows a large cell infiltrate of $iNOS^{+}$ cells into the s.c. area of inflamed skin (OXd4). (*D*) Mice implanted with $iNOS^{-/-}$ macrophages maintain strong lymphatic contractions compared with control. □, WT macrophage, $n = 8$; ■, $iNOS^{-/-}$ macrophage, $n = 8$. $^{*}P < 0.05$. *P* values are listed in Table S1. Error bars show SEM.

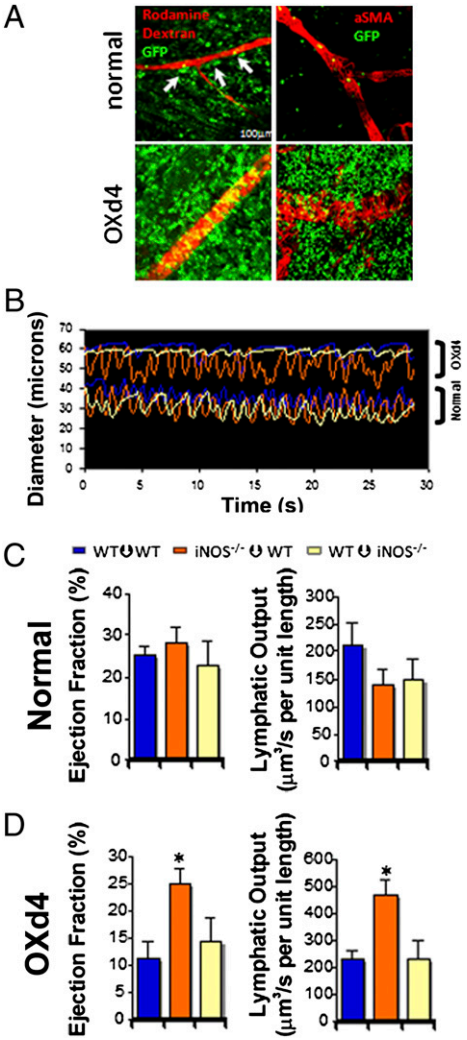

Fig. 3. Bone marrow-derived cells regulate lymphatic contraction during inflammation through iNOS. (*A*) BMDCs closely interact with lymphatic vessels during normal conditions (arrows). After the immunization, massive accumulation of BMDCs around lymphatic vessels occurs [green GFP^{+} BMDCs; red, rhodamine-dextran lymphangiography (*Left*) or αSMA^{+} cells (*Right*)]. (*B*) Representative lymphatic vessel contraction curves demonstrate that $iNOS^{-/-}$ to WT BMT mice maintain strong lymphatic contraction during inflammation whereas it is impaired in WT to $iNOS^{-/-}$ or WT to WT mice (*Upper*). On the other hand, there is no difference among the groups under normal conditions (*Lower*). (*C* and *D*) Lymphatic contraction analyses during (*C*) normal and (*D*) inflammatory conditions. ■, WT–WT normal, $n = 8$, OXd4, $n = 7$; ■, $iNOS^{-/-}$–WT normal, $n = 8$, OXd4, $n = 9$; ■, WT–$iNOS^{-/-}$ normal, $n = 8$, OXd4, $n = 8$. $^{*}P < 0.05$. *P* values are listed in Table S1. Error bars show SEM.

lation (Fig. 5 *A* and *B*). Accordingly, we observed reduced DC accumulation in draining OXd4 LNs (Fig. 5*C* and Fig. S7*A*) but not in OXd9 LNs. Next, we tested the functional significance of the attenuated lymphatic contraction and reduced DC accumulation by injecting the self-antigen myelin oligodendrocyte glycoprotein peptide 35–55 (MOG), which induces experimental autoimmune encephalomyelitis (EAE) (a mouse model of multiple sclerosis) (Fig. S7*B*). Clinical signs of EAE were prevented only if MOG was injected during the period of reduced lymphatic contraction (OXd2), not when injected after lymphatic contraction was recovering (OXd7) (Fig. 5*D*). The clinical signs were further reflected in the extent of LN size and the CNS cellular infiltrate (Fig. S7*C*). Finally, we tested the ability of dendritic cells isolated 24 h after MOG injection on OXd3 or OXd7 to stimulate a MOG-specific T-cell (2D2) response ex vivo. We found that antigen-bearing DCs are reduced in OXd3 LNs even though DCs isolated at OXd3 are functional and capable of correctly presenting MOG (Fig. S7*D*). Thus, the attenuated lymphatic vessel function prevented autoreactive T-cell activation and protected against autoimmune disease.

Discussion

The results from our studies of physiological and inflammatory conditions seem contradictory and reveal that the microenvironment surrounding collecting lymphatic vessels is a critical determinant of lymphatic function. Under physiological conditions, removing NO produced by eNOS in endothelial cells caused a reduction in contraction strength, whereas under inflammatory conditions removing NO produced by iNOS in BMDCs increased contraction strength. However, it is important to note that the temporal and spatial gradients of NO, in addition

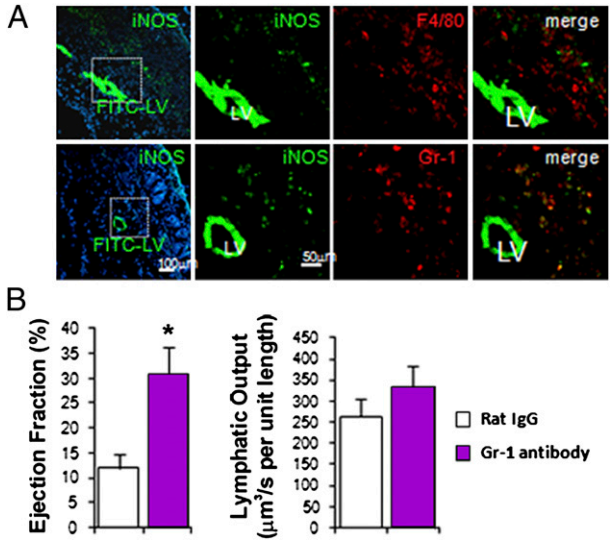

Fig. 4. Gr-1 cells are the major iNOS-expressing cells that suppress lymphatic contraction during the OX-induced edema. (*A*) *iNOS*-expressing cells surround the lymphatic vessel, which is highlighted with FITC-Lectin (green, LV). iNOS is stained with FITC-labeled antibody (green, punctuate stain). *Upper*, F4/80; *Lower*, Gr-1 (red). (*B*) Gr-1 antibody treatment maintains stronger lymphatic contraction compared with Rat IgG control antibody treatment. □, Control IgG, $n = 8$; ■, Gr-1 antibody, $n = 9$. $^*P < 0.05$.

to total amount, are critical to its ultimate function (16, 29). Under physiological conditions, eNOS produces NO in lymphatic endothelial cells at specific locations and times during a contraction cycle (22), which facilitates diastolic filling. We propose that during inflammation, excessive amounts of NO produced by iNOS in infiltrated BMDCs overwhelm the spatial and temporal NO gradients produced by eNOS (Fig. 6), thus inhibiting contraction. Furthermore, iNOS-derived NO may cause continuous relaxation of peri-lymphatic SMCs, increasing vessel diameter, reducing inotropy, and thus reducing contraction strength. Collectively, these results indicate when and where NO is produced during physiological and pathological conditions determine its ultimate effect on lymphatic contraction.

Systemic Compensation for Reduced Strength of Lymphatic Contraction. We measured reduced lymphatic contraction strength and increased lymphatic diameter in eNOS$^{-/-}$ mice and after NOS inhibition in WT mice. Because NO is a vessel relaxation factor, we expected to observe a constricted lymphatic vessel after its blockade. Surprisingly, we measured larger lymphatic diameters in NOS-inhibited animals compared with control animals, which is different from temporary inhibition in rat (22). However, lymph output in L-NMMA, *eNOS*$^{-/-}$, and WT mice was not significantly different, suggesting that increases in lymphatic diameter and contraction frequency may result from systemic compensation for the reduced strength of contraction to maintain fluid balance. In fact, we did observe a reduced ejection fraction and lymph output when activated macrophages were injected acutely (2 h), leaving little time for systemic compensation (Fig. 2*D*). Although other molecules have been implicated in lymphatic contraction (11, 30–35), the molecular mechanisms underlying this compensation have yet to be elucidated in our model system.

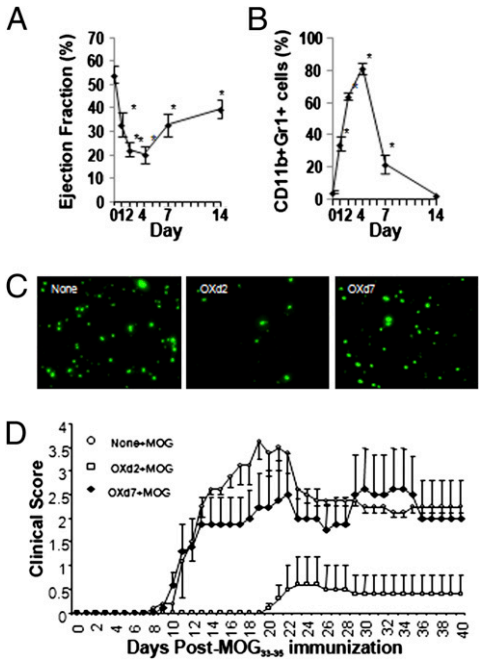

Fig. 5. Induction of EAE is prevented temporarily after oxazolone skin painting due to reduced MOG accumulation in the draining lymph node. Dynamics of (*A*) lymphatic contraction and (*B*) Gr-1$^+$ cell accumulation during OX contact sensitization are shown at times between 0 and 14 d. (*C*) Reduction of FITC-positive DC accumulation in LN when microspheres were injected at OXd2, but recovered if injected at OXd7. (*D*) EAE clinical score shows protection from autoimmune response when MOG was injected at OXd2, but not at OXd7.

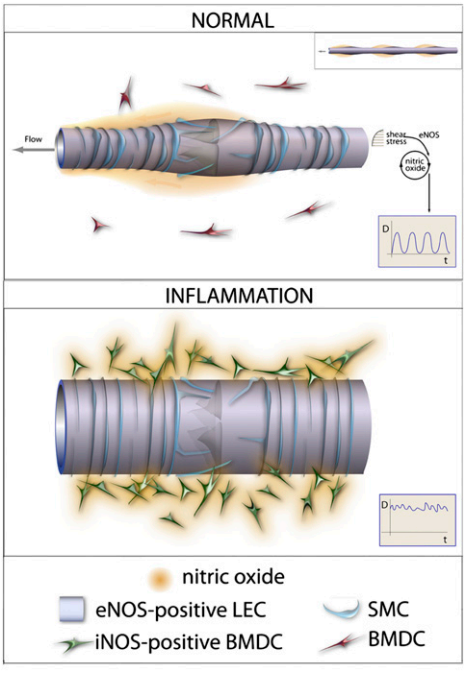

Fig. 6. Proposed mechanisms of NOS regulation of lymphatic contraction during normal and inflammatory conditions. Under normal conditions, eNOS in lymphatic endothelial cells produces temporal and spatial NO gradients that maintain robust lymphatic contractions (*Inset*). During inflammation, NO production from iNOS in infiltrated BMDCs overwhelms the NO gradients produced by eNOS. BMDC-derived NO causes excessive relaxation of collecting lymphatic vessels, thereby reducing the strength of lymphatic contraction (*Inset*).

Implications of Lymphatic Contraction for Immune Response. Our study revealed a unique function of myeloid-derived cells in regulating lymphatic function and has broad implications for immune regulation in pathological conditions. To initiate an immune response, antigen and antigen-presenting cells arrive in the draining LN within 24 h after antigen encounter (36, 37). Shortly after this initial period, we propose that myeloid cells accumulate at the inflammatory site and inhibit collecting lymphatic function, suppressing further immune response to self-antigen by reducing antigen transport to the lymph node. This mechanism is advantageous when suppressing a response by self-antigen–specific lymphocytes during an ongoing immune or inflammatory response. However, this mechanism of tolerance may be usurped by cancer cells or chronic infections, which can produce similar inflammatory conditions (1–3, 5, 38, 39) to inhibit lymphatic contractions. Thus, in addition to immune suppressor cells (myeloid-derived suppressor cells or regulatory T cells) (40, 41) and alterations of the microenvironment in inflamed LNs (cell components and vasculature, cytokine, and chemokine expression) (2, 42), the disruption of lymphatic function might provide another mechanism of immune evasion by cancer or bacteria. Furthermore, manipulation of lymphatic function may decrease the rate of rejection of transplanted organs (6). Using our unique methods, we are able to further study the important implications of lymphatic contraction on immune function during normal and disease states.

Materials and Methods

See *SI Materials and Methods* for further descriptions.

Lymphatic Contraction Model. Briefly, mice were anesthetized with ketamine/xylazine (10/100 mg/kg i.p.) and 2 μL of 2% FITC-Dextran (2 M Da; Molecular Probes) was injected in the footpad. Five minutes later, the leg skin and underlying connective tissue near the popliteal afferent lymphatic vessel were carefully removed using sterile microsurgical dissection. The leg of the mouse was immobilized and time-lapse images (360 images separated by 80 ms) were taken with an inverted fluorescence microscope (Olympus) driven by OpenLab software (Improvision). The motion of the lymphatic vessels was limited in the valve area (Movie S15). We therefore took images only of the intravalvular lymphangion area for the analysis of lymphatic contraction where we observed consistent strong contraction (Movie S16 and Fig. S8). For each mouse, we imaged two to three lymphatic segments and took images every 15 min for four time points. We used average results collected from a single mouse to represent the lymphatic contraction parameters for that animal.

Oxazolone Immunization Through Skin Painting. For the lymphatic pumping study, 100 μL of 4% oxazolone (Sigma) in acetone was applied topically to all of the skin area surrounding each leg, but not touching the skin over the paw. This procedure led to an inflammatory reaction and edema surrounding the PLV, but there was not direct skin inflammation or obvious edema in the paw of the mouse. Any footpad edema that occurs represents the reduction in function of downstream lymphatics in the region of the OX painting in the leg. For EAE study, 50 μL of 4% oxazolone in acetone was applied at each of the inguinal and brachial lymph node areas (200 μL per mouse).

Gr-1 Antibody Blockade. Rat anti-Gr-1 antibody (Biolegend) at 10 mg/kg was injected i.p. 1 d before and 2 d after oxazolone application.

Statistical Analysis. Description and discussion of the analysis of lymphatic contraction curves can be found in *SI Materials and Methods*. Comparison between groups was made using Student's *t* test or ANOVA with Tukey's HSD posthoc test as appropriate. Statistical significance was considered as $P < 0.05$. Error bars are SEM.

ACKNOWLEDGMENTS. We thank Qingcong Lin, Paul L. Huang, Peigen Huang, and Ravi Mylvaganam as well as the Massachusetts General Hospital Flow Cytometry Core for reagents and expertise. This study was supported in part by a Tosteson Postdoctoral Fellowship from the Massachusetts Biomedical Research Corporation (to S.L.); a Charles A. King Trust Fellowship Award (to S.L.); National Institutes of Health Grant R01 DK57731 and Multiple Sclerosis Society Grants RG 4126-A-7 (to N.H.R.) and U01-CA084301 (to R.S.K.); and National Cancer Institute Grants R01-CA96915 (to D.F.), R01-CA85140, R01-CA115767, R01-CA126642 (to R.K.J.), P01-CA80124 (to R.K.J., D.F., and L.L.M.), and K99-CA137167 (to T.P.P.).

1. Jeon BH, et al. (2008) Profound but dysfunctional lymphangiogenesis via vascular endothelial growth factor ligands from CD11b+ macrophages in advanced ovarian cancer. *Cancer Res* 68:1100–1109.
2. Liao S, Ruddle NH (2006) Synchrony of high endothelial venules and lymphatic vessels revealed by immunization. *J Immunol* 177:3369–3379.
3. Hoshida T, et al. (2006) Imaging steps of lymphatic metastasis reveals that vascular endothelial growth factor-C increases metastasis by increasing delivery of cancer cells to lymph nodes: Therapeutic implications. *Cancer Res* 66:8065–8075.
4. Angeli V, et al. (2006) B cell-driven lymphangiogenesis in inflamed lymph nodes enhances dendritic cell mobilization. *Immunity* 24:203–215.
5. Padera TP, et al. (2002) Lymphatic metastasis in the absence of functional intratumor lymphatics. *Science* 296:1883–1886.
6. Kerjaschki D, et al. (2004) Lymphatic neoangiogenesis in human kidney transplants is associated with immunologically active lymphocytic infiltrates. *J Am Soc Nephrol* 15: 603–612.
7. Isaka N, Padera TP, Hagendoorn J, Fukumura D, Jain RK (2004) Peritumor lymphatics induced by vascular endothelial growth factor-C exhibit abnormal function. *Cancer Res* 64:4400–4404.
8. Schmid-Schönbein GW (1990) Microlymphatics and lymph flow. *Physiol Rev* 70: 987–1028.
9. Skalak TC, Schmid-Schönbein GW, Zweifach BW (1984) New morphological evidence for a mechanism of lymph formation in skeletal muscle. *Microvasc Res* 28:95–112.
10. von der Weid PY, Zawieja DC (2004) Lymphatic smooth muscle: The motor unit of lymph drainage. *Int J Biochem Cell Biol* 36:1147–1153.
11. Breslin JW, et al. (2007) Vascular endothelial growth factor-C stimulates the lymphatic pump by a VEGF receptor-3-dependent mechanism. *Am J Physiol Heart Circ Physiol* 293:H709–H718.
12. Eisenhoffer J, Yuan ZY, Johnston MG (1995) Evidence that the L-arginine pathway plays a role in the regulation of pumping activity in bovine mesenteric lymphatic vessels. *Microvasc Res* 50:249–259.
13. Gasheva OY, Zawieja DC, Gashev AA (2006) Contraction-initiated NO-dependent lymphatic relaxation: A self-regulatory mechanism in rat thoracic duct. *J Physiol* 575: 821–832.
14. Johnston MG, Hay JB, Movat HZ (1979) Kinetics of prostaglandin production in various inflammatory lesions, measured in draining lymph. *Am J Pathol* 95:225–238.
15. Ohhashi T, Mizuno R, Ikomi F, Kawai Y (2005) Current topics of physiology and pharmacology in the lymphatic system. *Pharmacol Ther* 105:165–188.
16. Fukumura D, Kashiwagi S, Jain RK (2006) The role of nitric oxide in tumour progression. *Nat Rev Cancer* 6:521–534.
17. Koller A, Mizuno R, Kaley G (1999) Flow reduces the amplitude and increases the frequency of lymphatic vasomotion: Role of endothelial prostanoids. *Am J Physiol* 277:R1683–R1689.
18. Shirasawa Y, Ikomi F, Ohhashi T (2000) Physiological roles of endogenous nitric oxide in lymphatic pump activity of rat mesentery in vivo. *Am J Physiol Gastrointest Liver Physiol* 278:G551–G556.
19. Bridenbaugh EA, Gashev AA, Zawieja DC (2003) Lymphatic muscle: A review of contractile function. *Lymphat Res Biol* 1:147–158.
20. Hagendoorn J, et al. (2004) Endothelial nitric oxide synthase regulates microlymphatic flow via collecting lymphatics. *Circ Res* 95:204–209.
21. Kajiya K, Huggenberger R, Drinnenberg I, Ma B, Detmar M (2008) Nitric oxide mediates lymphatic vessel activation via soluble guanylate cyclase alpha1beta1-impact on inflammation. *FASEB J* 22:530–537.
22. Bohlen HG, Wang W, Gashev A, Gasheva O, Zawieja D (2009) Phasic contractions of rat mesenteric lymphatics increase basal and phasic nitric oxide generation in vivo. *Am J Physiol Heart Circ Physiol* 297:H1319–H1328.
23. Lahdenranta J, et al. (2009) Endothelial nitric oxide synthase mediates lymphangiogenesis and lymphatic metastasis. *Cancer Res* 69:2801–2808.
24. Mizuno R, Koller A, Kaley G (1998) Regulation of the vasomotor activity of lymph microvessels by nitric oxide and prostaglandins. *Am J Physiol* 274:R790–R796.
25. von der Weid PY, Zhao J, Van Helden DF (2001) Nitric oxide decreases pacemaker activity in lymphatic vessels of guinea pig mesentery. *Am J Physiol Heart Circ Physiol* 280:H2707–H2716.
26. Bernard C, et al. (1992) Activated macrophages depress the contractility of rabbit carotids via an L-arginine/nitric oxide-dependent effector mechanism. Connection with amplified cytokine release. *J Clin Invest* 89:851–860.
27. Balligand JL, et al. (1993) Abnormal contractile function due to induction of nitric oxide synthesis in rat cardiac myocytes follows exposure to activated macrophage-conditioned medium. *J Clin Invest* 91:2314–2319.
28. Medeiros R, Figueiredo CP, Passos GF, Calixto JB (2009) Reduced skin inflammatory response in mice lacking inducible nitric oxide synthase. *Biochem Pharmacol* 78: 390–395.
29. Kashiwagi S, et al. (2008) Perivascular nitric oxide gradients normalize tumor vasculature. *Nat Med* 14:255–257.

30. Sakai H, Ikomi F, Ohhashi T (1999) Effects of endothelin on spontaneous contractions in lymph vessels. *Am J Physiol* 277:H459–H466.
31. Fox JL, von der Weid PY (2002) Effects of histamine on the contractile and electrical activity in isolated lymphatic vessels of the guinea-pig mesentery. *Br J Pharmacol* 136: 1210–1218.
32. Chan AK, von der Weid PY (2003) 5-HT decreases contractile and electrical activities in lymphatic vessels of the guinea-pig mesentery: Role of 5-HT 7-receptors. *Br J Pharmacol* 139:243–254.
33. Hosaka K, Mizuno R, Ohhashi T (2003) Rho-Rho kinase pathway is involved in the regulation of myogenic tone and pump activity in isolated lymph vessels. *Am J Physiol Heart Circ Physiol* 284:H2015–H2025.
34. Kousai A, Mizuno R, Ikomi F, Ohhashi T (2004) ATP inhibits pump activity of lymph vessels via adenosine A1 receptor-mediated involvement of NO- and ATP-sensitive K+ channels. *Am J Physiol Heart Circ Physiol* 287:H2585–H2597.
35. Li X, Mizuno R, Ono N, Ohhashi T (2008) Glucose and glucose transporters regulate lymphatic pump activity through activation of the mitochondrial ATP-sensitive K+ channel. *J Physiol Sci* 58:249–261.
36. Mempel TR, Henrickson SE, Von Andrian UH (2004) T-cell priming by dendritic cells in lymph nodes occurs in three distinct phases. *Nature* 427:154–159.
37. Sixt M, et al. (2005) The conduit system transports soluble antigens from the afferent lymph to resident dendritic cells in the T cell area of the lymph node. *Immunity* 22: 19–29.
38. Choi WS, Chang MS, Han JW, Hong SY, Lee HW (1997) Identification of nitric oxide synthase in Staphylococcus aureus. *Biochem Biophys Res Commun* 237:554–558.
39. Gusarov I, Shatalin K, Starodubtseva M, Nudler E (2009) Endogenous nitric oxide protects bacteria against a wide spectrum of antibiotics. *Science* 325: 1380–1384.
40. Gabrilovich DI, Nagaraj S (2009) Myeloid-derived suppressor cells as regulators of the immune system. *Nat Rev Immunol* 9:162–174.
41. Littman DR, Rudensky AY (2010) Th17 and regulatory T cells in mediating and restraining inflammation. *Cell* 140:845–858.
42. Mueller SN, et al. (2007) Regulation of homeostatic chemokine expression and cell trafficking during immune responses. *Science* 317:670–674.